Subgap absorption study of chemical vapor deposited thin diamond films

U. Zammit, K. N. Madhusoodanan, M. Marinelli, F. Mercuri, and S. Foglietta
Dipartimento di Ingegneria Meccanica, Università di Roma ''Tor Vergata,'' via di Tor Vergata 00133 Rome, Italy and I.N.F.M., Unità di Roma II ''Tor Vergata,'' Rome, Italy
(Received 22 September 1997)

Subgap absorption studies were carried out on chemical vapor deposited diamond very thin films (0.25–1.60 μm) over a spectral range extending deep into the subgap region of the material (0.3–4.4 eV). The subgap absorption was confirmed to be basically associated with the relative graphitic carbon content which increased with methane concentration in the gas mixture but decreased when the Si substrate temperature was raised from 860 °C to 950 °C. No systematic smaller grain size was found in those films with larger graphitic carbon content. Texturing along the $\langle 110 \rangle$ direction is shown to lead to greater diamond phase purity than along the $\langle 100 \rangle$ direction. The convolution integral involving only π electronic gap states associated with graphitic carbon is found to be sufficient to reproduce the absorption spectra of the films as well as that of type-IIa single crystals down to the lowest-energy region not affected by multiphonon absorption. [S0163-1829(98)02907-5]

INTRODUCTION

Diamond is a wide gap semiconductor and should show both electrical insulator behavior and negligible optical absorption in the visible–near-IR spectral region. Actually diamond exhibits absorption and some electrical conductivity due to the presence of defects in the material. To understand such behavior it is necessary to study the effect of the various kinds of defects on the electronic density of states in the band gap of the material. Subgap optical-absorption techniques are sensitive to all kind of defects as pointed out in the case of Si.[1,2] Thin diamond films grown by chemical vapor deposition (CVD) have led to new applications in the field of thin film devices and protective coatings and to the need of research activity to characterize the material. When considering subgap optical-absorption measurements in thin films of CVD diamond, two main requirements should be borne in mind. It should be very sensitive due to the often-limited thickness of the films and the low absorption of the subgap spectral region. Moreover, CVD diamond samples generally present light scattering due to their polycrystalline structure with the grain size depending on the growth conditions. The adopted technique should thus be basically insensitive to light scattering.

Photothermal deflection spectroscopy[1] PDS is a technique which does fulfill both such requirements and thus looks particularly attractive for subgap absorption measurements in CVD diamond thin films. PDS absorption measurements have recently been reported in CVD diamond films of thickness 20–100 μm in the spectral range 0.9–4.4 eV.[3,4] These show that the subgap absorption over such a range is basically associated with sp^2 carbon and that such graphitic carbon content increases with the CH_4 concentration in the gas mixture and/or the Si substrate temperature, leading to larger subgap absorption levels. This trend was associated with the observed reduction in mean grain size of the material which was also found to occur with the above-mentioned changes, since the grain boundary area, a possible preferential site for graphitic carbon, would correspondingly increase. Finally, the absorption spectra in the subgap region, showing a shoulder feature down to about 1 eV, could be fitted with a convolution integral where the initial and final electronic states were, respectively, Gaussian-like bands of localized bonding and antibonding π states associated with the sp^2 carbon.

In this paper we have applied the PDS technique to the study of the subgap absorption of very thin films (0.25–1.60 μm) of CVD diamond, thus monitoring them from the early stages of growth. A recently described large range PDS setup[5] enabled the extension of the investigated spectral range much farther into the subgap region of the material (0.35–4.50 eV) as compared with the previous studies. Measurements were performed also on thicker samples (12 μm) in order to detect inhomogeneities in the film properties as a function of thickness. The spectra of diamond IIa and Ib single crystalline samples are also reported and discussed.

Considerably larger absolute absorption values than the ones reported in Refs. 3 and 4 were obtained for films grown under similar conditions and for IIa bulk diamond. Lower values in the film absorption may be caused by the larger film thickness, as shown below, but the discrepancy may also be explained in terms of the adopted calibration procedures. The subgap absorption and therefore the relative graphitic carbon content in the film is found to increase with CH_4 content, as in the above-mentioned work, but the increase in substrate temperature from 860 °C to 950 °C leads to decreasing subgap absorption. Moreover, no systematic connection between film grain size and relative content of graphitic carbon has been found in the present study. The relative graphitic carbon content was found to be affected also by the texturing conditions. $\langle 110 \rangle$ texturing is shown to lead to greater diamond phase purity than $\langle 100 \rangle$ texturing. Finally it is shown that a convolution integral involving only π electronic gap states associated with the sp^2 carbon is sufficient to fit the shoulder feature down to about 1 eV, typical of graphitic carbon films, as well as the region found at lower energies and not previously investigated. The same convolution integral could successfully reproduce also the subgap absorption continuum of type-IIa diamond single crystals.

EXPERIMENT

Diamond films were grown on a 1×1-cm^2 polished p-type (100) Si substrate. A two-step deposition process was

TABLE I. Deposition conditions and characteristics of CVD diamond films.

Sample	Pressure (Pa)	Temperature (°C)	CH_4 (%)	MW power (W)	Deposition time (min)	Thickness (μm)
860-04	5000	860	0.4	300	90	0.25
860-08	5000	860	0.8	300	90	0.45
860-20	5000	860	2.0	300	90	1.0
860-20-12	5000	860	2.0	300	600	12.0
950-04	5000	950	0.4	300	90	0.5
950-08	5000	950	0.8	300	90	0.95
950-20	5000	950	2.0	300	90	1.6

adopted for all the samples investigated in this work. A 2-min biasing pre-treatment with -200 V applied voltage and 5% CH_4 volume concentration, in a CH_4-H_2 mixture, was used to promote a uniform and highly reproducible nucleation on the Si substrates. The growth time of the following deposition step was kept fixed at 1.5 h for all the films (except for the 12-μm-thick one where it was 10 h) such that the growth rate for the investigated films ranged between 0.3 and 1.2 μm/h. The thickness of each film, measured with scanning electron microscopy (SEM) of the cross sections, depends on the growth conditions and is reported in Table I together with the other growth parameters. The films were grown on substrates at 860 °C and 950 °C and CH_4 concentrations which ranged between 0.4% and 2.0%.

The absorption measurements were performed between 4.50 and 0.35 eV (280 and 3500 nm) using the wide range PDS setup described in Ref. 5. To have access to the spectral region above the Si substrate band gap, after the deposition the Si substrate was removed by a chemical etch in HNO_3/HF/CH_3CO_2H solution and the films were placed on 300-μm-thick sapphire substrates to which they perfectly adhered after drying, leaving no residual gap. Interference-induced oscillations were obtained in the PDS signal spectra of the thinnest and less absorbing samples due to the differences of refractive index values between the film and the sapphire. The ratio of simultaneously determined transmittance and PDS signal spectra enabled the elimination of the oscillations as previously described.[2,5,6]

Measurements were also performed on 200-μm-thick type-IIa and -Ib single crystalline diamond samples.

RESULTS AND DISCUSSION

Calibration of absorption values

Figure 1 shows the absorption spectra for some CVD diamond films while Fig. 2 reports the results for the bulk samples. The films show considerable larger absorption. Though there is qualitative agreement of the relative profile of the spectra of these CVD diamond films with the ones reported earlier,[3,4] the absolute absorption values are up to one order of magnitude larger. Moreover, the absolute absorption values of the IIa diamond are two orders of magnitude larger (at 3 eV) than reported in Refs. 3 and 4. Lower values in the films may be caused by the larger film thickness, as shown later on, but a large discrepancy in the case of the IIa diamond still remains unexplained.

Calibration is necessary to obtain the absolute absorption values from the PDS signal spectrum. Transmission measurements cannot be used for calibration on thin CVD diamond films because of light scattering and because of the very small absorptance of the films which makes the transmission values dependent primarily on the overall film reflectance. A straightforward procedure can be adopted when optical saturation (full absorption of the nonreflected component of the incident light) is achieved in some part of the spectrum since the PDS signal S is proportional to the sample absorptance:[1] $S=S_{\mathrm{sat}}(1-e^{-\beta l})$ where S_{sat} is the signal in the saturation region, β is the absorption coefficient, and l the film thickness. For most of the films reported in Refs. 3 and 4 and for the IIa diamond samples optical saturation was not obtained in any part of the investigated spectral region due to the limited film absorptance. In those references the calibration for the nonsaturating films was performed by comparing the PDS signal value obtained at one particular wavelength with that of another diamond film with the same geometric characteristics (lateral dimensions and thickness) but a larger component of sp^2 carbon so that it showed optical saturation at the selected wavelength. However, the PDS signal depends on the thermal diffusivity value of the sample which in turn is strongly affected by the structure, the sp^2 carbon content,[7] as well as other impurities in the film. This effect combined with possible nonperfect reproducibility of the sample positioning with respect to the probe beam may lead to considerable uncertainty in the calibration procedure. In the present work the PDS signal for each film was calibrated against the one obtained for the

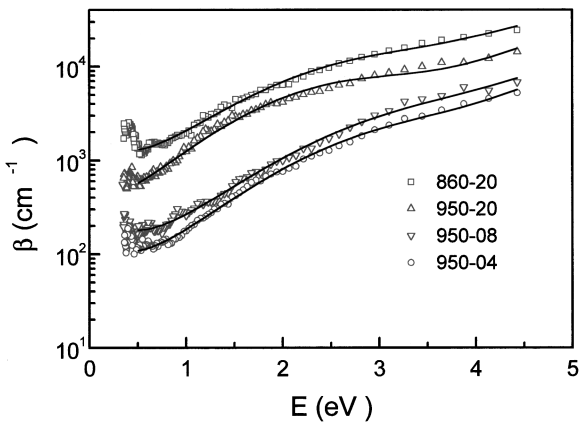

FIG. 1. Absorption spectra for CVD diamond films grown at 950 °C and at 860 °C (see Table I). The continuous lines represent the best fit results obtained with the convolution integral described in the text.

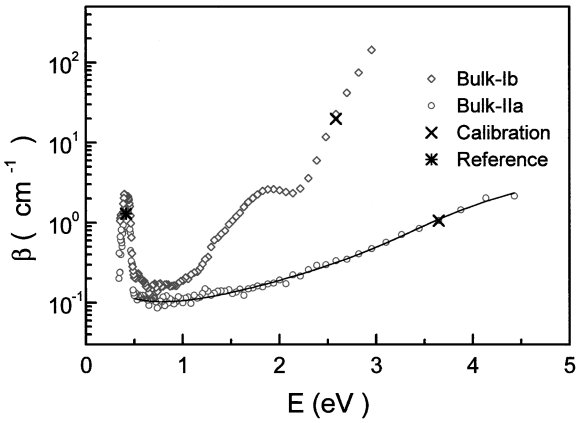

FIG. 2. Absorption spectra for bulk single crystalline diamond samples. The × symbols and asterisk represent calibration and reference values (see text). The continuous lines represent the best fit results obtained with the convolution integral described in the text.

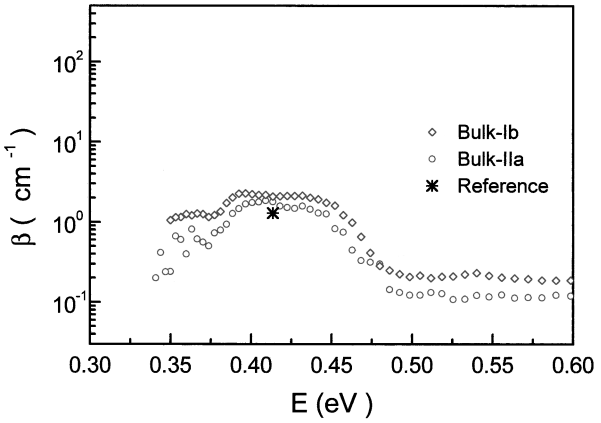

FIG. 3. Details of the spectra of the samples reported in Fig. 2 in the diamond three-phonon absorption region.

same film after it was made opaque by deposition of a ''thin'' surface layer of carbon black. In such a way both the geometrical parameters and the thermal diffusivity of the film and substrate remained unchanged during the two measurements. Moreover, the sample position reproducibility in the PDS cell with respect to the probe beam was ensured by simply placing the sample several times in the cell and checking for corresponding variations in the PDS signal. The values were reproducible within less than 5%. An adequate thickness of the carbon black film is crucial for a successful calibration. It must not be too thick otherwise the porosity of the layer would provide a thermal barrier for the heat generated by the light absorption to diffuse into the sample. The PDS signal would then be artificially increased (up to a factor of 10). When the layer is too thin it would not ensure optical saturation. An adequate thickness of the layer was determined to be the one that corresponded to 1–1.3 neutral density filter. To check this procedure we have compared the absorption values calculated at 2.6 eV with two different calibrating procedures for the diamond Ib sample which showed optical saturation in the region above 3 eV, by calibrating against the PDS signal value in the saturation region (diamond in Fig. 2) and by calibrating with the above-described procedure (× symbol in Fig. 2). The close proximity of the two values confirms the reliability of the procedure adopted. Furthermore, the cross-checking went further when we determined the absorption spectrum for diamond IIa using the calibration point at 3.65 eV (× symbol in Fig. 2) obtained with the above-mentioned procedure. We then compared the absorption values obtained in the three-phonon absorption band region ($0.37<E<0.47$ eV), shown in greater detail in Fig. 3, with the value which had been obtained for diamond IIa in Ref. 8 (asterisk). Once again the two values are in close agreement.

Effects of growth conditions

In Fig. 1 the absorption spectra for the diamond films grown at 950 °C with increasing methane concentration are reported together with the one grown at 860 °C with 2% methane concentration. Qualitatively the shoulder feature observed in the spectra down to about 1 eV is very similar to that reported in Ref. 4 and, as stated therein, also to those observed in *a*-C:H.[9,10] Moreover, in Ref. 4 the subgap absorption increase is shown to be accompanied by a corresponding increase in the graphitic carbon component of the Raman signal. The continuous lines in the figure represent the fits obtained with convolution integrals based on electronic density of states in the gap characteristic of graphitic carbon.[4] This indicates that the subgap absorption is mainly associated with the graphitic carbon component in the films.

In Fig. 1 the absorption values, and therefore the relative sp^2 carbon content in the films, are shown to increase with methane concentration during the growth. This is also true for the films grown at 860 °C (Fig. 4). These results are in agreement with those reported in Refs. 3 and 4 and are also consistent with the diamond domain in Bachmann and coworkers' C-O-H phase diagram,[11] which shows that increasing the relative methane content in the gas mixture induces a shift towards the graphitic carbon growth region. Figures 1 and 4 show that a decrease in the substrate temperature also leads to an increase of the relative graphitic carbon content in the films. The opposite result was obtained in the work reported in Refs. 3 and 4 where, however, the films had random growth and the maximum substrate temperature of 900 °C was probably insufficient to achieve ⟨110⟩ texturing

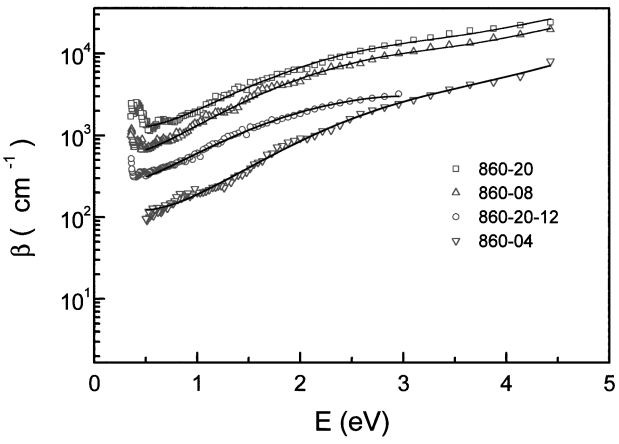

FIG. 4. Absorption spectra for CVD diamond films grown at 860 °C (see Table I). The continuous lines represent the best fit results obtained with the convolution integral described in the text.

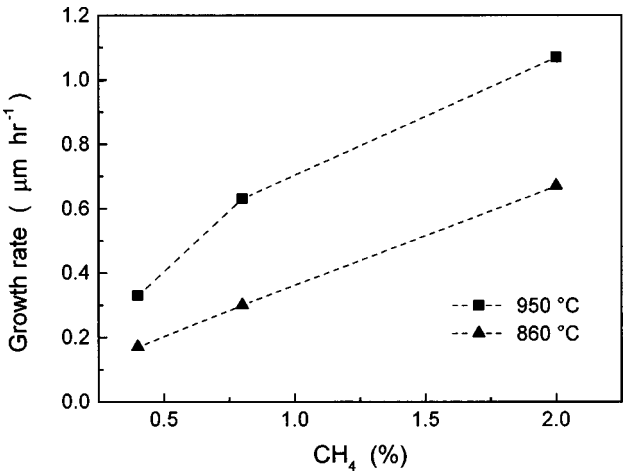

FIG. 5. Growth rate of the CVD diamond films as a function of CH_4 concentration and substrate temperature. The broken lines are guides for the eye.

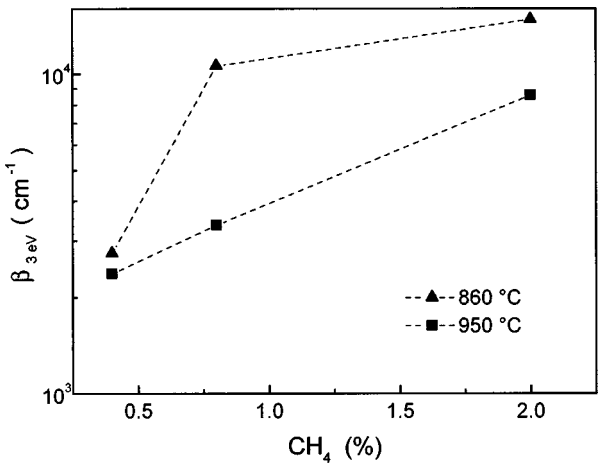

FIG. 6. Subgap absorption at 3 eV for the CVD diamond films as a function of CH_4 concentration and substrate temperature. The broken lines are guides for the eye.

which, as discussed later on, may play an important role in terms of the sp^2 carbon content in the film. In Refs. 3 and 4 a systematic correlation between the larger relative graphitic carbon content and a smaller film mean grain size was observed. The increase in sp^2 carbon content was thus explained with the increase in available grain boundary area, a possible preferential site for sp^2 carbon. SEM observations performed on our films show that a smaller mean grain size is indeed associated with the larger sp^2 carbon content obtained in the films grown at lower substrate temperature but this is not the case when the larger sp^2 carbon content is obtained by increasing the methane concentration at either temperature where the mean grain size remains substantially unchanged. It is not only the grain boundary area which may affect the overall content of sp^2 carbon in the films but, presumably, also other factors such as the obtained structure and direction as discussed below.

Figure 4 also reports the spectrum for a 12-μm film grown with the same conditions as one of the thinner films. The absorption values are smaller than those of the corresponding thinner film. The measured absorption corresponds to an effective value averaged over the entire thickness of the film which is known to be more defective and with a larger graphitic content during the earlier stages of the growth. In the thicker films, the average value includes subsequent layers of material which grow with a lower graphitic carbon content thus leading to a lower effective absorption coefficient.

The results reported in Figs. 1 and 4 and some of those reported in Table I are summarized in Figs. 5 and 6 which show, respectively, the film growth rate and the subgap absorption at 3 eV for increasing methane concentration and different substrate temperatures. These show that an increase in the film growth rate is obtained both by increasing the methane concentration and/or upon increasing the substrate temperature from 860 °C to 950 °C. The CH_4 concentration increase leads to films with larger relative graphitic carbon content. This may be explained by considering that, upon methane increase, the gas composition is changed such as to shift conditions away from the boundary of the no growth region towards the one of the graphitic carbon growth region within the diamond domain of the C-H-O phase diagram.[11] This induces an increase in the growth rate of the film but at the expense of the diamond phase purity. On the other hand, when the substrate temperature is increased to 950 °C the increase in growth rate is accompanied by a larger diamond phase purity. This justification of this result, not as yet explored in detail, requires the consideration of other factors like the growth structure and direction.

The films used in this work had been previously studied by x-ray diffraction (XRD), cathotoluminescence (CL), Raman spectroscopy, as well as SEM.[12] The XRD studies revealed that the samples grown at 860 °C showed an increasing tendency to texturing along the ⟨100⟩ direction with increasing CH_4 concentration for values exceeding 1–1.2%, random polycrystalline material being obtained for methane concentration values of 0.4% and 0.8%. The samples grown at 950 °C, on the other hand, showed pronounced texturing along the ⟨110⟩ direction for methane concentration of 2% but even for lower values ''weak'' texturing is still obtained since the ratios of the intensities of the {220} and {111} x-ray diffraction peaks remain three to five times larger than the value of about 0.1 typical for a randomly oriented material. It has been shown in the literature[13] that the texturing behavior of CVD diamond films is governed by the value of the parameter $\alpha=\sqrt{3}V_{100}/V_{111}$ where V_{100} and V_{111} are, respectively, the growth velocities of the {100} and {111} crystal facets. It has also been shown that when the growth conditions are such that the value of α approaches its maximum value of 3, texturing along the ⟨100⟩ directory is achieved while smaller values of α shift the texturing direction towards the ⟨110⟩ direction. It is finally shown that the value of α tends to 3 for methane concentrations exceeding about 1.5% with a substrate temperature of 800 °C but that α decreases once the substrate temperature is larger than about 900 °C, consistently with the texturing behavior reported in this work.

The growth of ⟨110⟩ textured diamond films is known to occur with a considerably larger rate than along other texturing or random directions. It has been proposed that the rate is enhanced by the formation of {111} twin defects on the {110} diamond growth surface, a process which provides low-energy sites for preferential bonding of the atoms on the

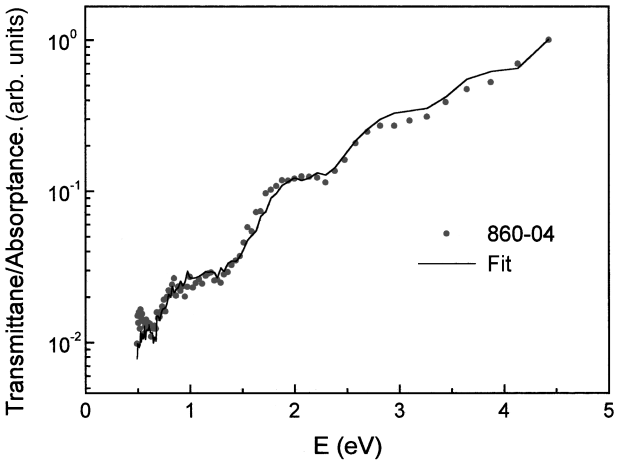

FIG. 7. Ratio of transmittance to absorptance for the 860-04 CVD diamond film (see Table I). The continuous line represents the best fit results obtained with a model described in the text.

{110} face.[14] This mechanism gives rise to structurally defective film growth with the presence of multiple twinning and stacking faults[12,14] but apparently with a *more efficient* growth of the diamond component with respect to the graphitic one than in the case of, for example, the ⟨100⟩ direction. This could be associated with the fact that {110} surfaces provide continuously available diamond bonding sites for in-plane propagation of the surface and strong bonding sites for the attachment of the subsequent layers.[14] This also leads to the larger mean grain size observed for the samples grown at 950 °C.

Another interesting feature of Fig. 6 is that the increase in the sp^2 carbon component at 860 °C seems to be stronger when the methane is increased from 0.4% to 0.8% than with the further increase to 2.0% while at 950 °C the increase in the sp^2 carbon component with methane is smoother at all concentrations. It seems that when the conditions are such that textured material is achieved variations in methane concentration lead to smaller change in relative graphitic carbon content in the film than when random growth is obtained.

The greater amount of structural defects observed in the films grown at 950 °C as detected by the CL investigations through the band *A* emission[12] is not reflected in larger subgap absorption in the spectra of Figs. 1 and 3 because the much larger absorption due to sp^2 carbon overshadows that associated with the defects. Moreover the Raman spectroscopy results of the films grown at 950 °C used in this work (Ref. 12) revealed no or negligible detection of the graphitic carbon component even for methane concentration of 2%. Subgap absorption spectroscopy proved to be more effective in this respect since it was able to detect it even in the thinnest films grown with 0.4% methane concentration.

Finally, Fig. 7 shows how it is possible with PDS measurements to discriminate between bulk absorption and that associated with interface graphitic carbon in thin films of CVD diamond. It has, in fact, been shown that complete cancellation of the interference oscillations in the ratio of the spectra of transmittance to PDS signal can be achieved in films when the bulk absorption is considerably larger than the one associated with defects localized on the film surface or interface.[15] The data in Fig. 7 represent the ratio of the two spectra obtained for the film grown at 860 °C with 0.4% methane concentration when illuminating it through the side which originally corresponded to the interface with the Si substrate. As shown, the interference oscillations do not cancel out completely. The continuous line corresponds to the fit to the data obtained with a two-layer model, one for the film and a much thinner one for the graphitic carbon-rich overlayer. The data can be reproduced with a ratio of surface to bulk absorptance of 30%. This result is not surprising since the first layers in the growth of CVD diamond are known to be rich in graphitic carbon and the bulk absorptance was small due to very small thickness and methane concentration. Growth with larger methane concentrations led to thicker films and a larger content of sp^2 carbon in the bulk and thus to basically complete cancellation of the ratio of the two spectra.

Density of states in the gap

The density of electronic states is assumed to originate fundamentally from the π electrons of graphitic carbon, following the detailed justification presented in Ref. 4, and from extended band states and band tail states from the σ electrons of carbon. When assuming the Tauc model for optical absorption,[16] an energy-independent momentum matrix element and the Velicky summation rule,[17] the optical-absorption coefficient is shown to depend on the convolution integral between initial (occupied) and final (empty) states of the electronic transition responsible for the photon absorption. Based on the qualitative similarity between the spectra obtained for CVD diamond and the ones observed for *a*-C:H it is argued that the transitions responsible for the observed features in the subgap region are fundamentally between the bonding and antibonding π states and between the bonding π states and the σ states in the conduction band and band tail. Unlike Ref. 4 we have not considered also the contribution of the transitions leading to the fundamental absorption in diamond as these would correspond to absorption around the fundamental band edge in diamond (5.45 eV) while the data in our spectra are limited to 4.5 eV.

The π bonding and antibonding electronic states are assumed to be symmetric about midgap energy[18] and are represented by two Gaussian functions.[4,19] The band tail states are described by an exponential function decaying into the band-gap region and the extended band states by a parabolic function.[4] The absorption coefficient β is then given by

$$\beta(E)=\frac{B_1}{E}\int \exp\left\{-\left[\varepsilon-\left(\frac{E_g}{2}-\frac{\Delta E}{2}\right)\right]^2\Big/2W^2\right\}$$
$$\times\exp\left\{-\left[(\varepsilon+E)-\left(\frac{E_g}{2}+\frac{\Delta E}{2}\right)^2\right]/2W^2\right\}d\varepsilon+\frac{B_2}{E}$$
$$\times\int \exp\left\{-\left[\varepsilon-\left(\frac{E_g}{2}-\frac{\Delta E}{2}\right)\right]^2\Big/2W^2\right\}$$
$$\times[(\varepsilon+E-E_c)^{1/2}+(E_m-E_c)^{1/2}$$
$$\times\exp[(\varepsilon+E-E_m)/E_0]]d\varepsilon,$$

where E is the photon energy, B_1 and B_2 are constants, ε is the energy coordinate, E_g the gap energy, ΔE the energy separation between the bonding and antibonding distributions of π states, W the width of such distributions, E_m the

TABLE II. Best fit values and statistical uncertainties of the fitting parameters of the convolution integrals.

Sample	E_g (eV) fixed	ΔE (eV)	W (eV)	E_m (eV)	E_0 (eV)	B_1 (cm^{-1})	B_2 ($cm^{-1}\,eV^{1/2}$)
860-04	5.45	3.8 ± 0.1	0.68 ± 0.06	6.5 ± 0.2	0.61 ± 0.08	$(6.1\pm3.3)\times10^3$	$(5.8\pm2.0)\times10^4$
860-08	5.45	3.60 ± 0.03	0.76 ± 0.01	6.8 ± 0.1	0.56 ± 0.03	$(2.1\pm0.2)\times10^4$	$(5.8\pm1.2)\times10^4$
860-20	5.45	3.4 ± 0.1	0.71 ± 0.02	6.5 ± 0.1	0.68 ± 0.04	$(2.3\pm0.6)\times10^4$	$(1.5\pm0.3)\times10^5$
860-20-12	5.45	3.5 ± 0.3	0.76 ± 0.09	6.2 ± 1.1	0.57 ± 0.65	$(0.74\pm0.18)\times10^4$	$(6.0\pm9.0)\times10^4$
950-04	5.45	3.80 ± 0.04	0.70 ± 0.01	6.4 ± 0.2	0.61 ± 0.02	$(0.47\pm0.05)\times10^4$	$(5.7\pm0.8)\times10^4$
950-08	5.45	3.8 ± 0.2	0.71 ± 0.08	6.5 ± 0.2	0.65 ± 0.10	$(0.66\pm0.40)\times10^4$	$(6.4\pm2.8)\times10^4$
950-20	5.45	3.4 ± 0.3	0.72 ± 0.01	5.5 ± 0.8	0.48 ± 0.40	$(1.9\pm0.2)\times10^4$	$(9.6\pm5.4)\times10^4$
Bulk-IIa	5.45	4.4 ± 0.2	0.40 ± 0.08	6.7 ± 0.2	0.78 ± 0.20	2.8 ± 3.0	23 ± 10

energy value where the parabolic conduction band starts decaying exponentially into a band tail distribution of states,[4] and E_0 is the Tauc energy and determines the slope of the decay of the band tail distribution. E_c, ε, and E_m are measured from the top of the valence band. Thus numerically E_c and E_g coincide. The form of the second integral looks different from the corresponding one used in Ref. 4 but it is equivalent to it once the boundary condition of continuity of the exponential distribution and the parabolic one at E_m is applied as described in Ref. 4.

The MINUIT routine for function minimization and error analysis routine of the CERN Library is used to fit the theoretical expression of the absorption coefficient to the experimental data. For each curve, data down to 0.6 eV were used for the fitting, that is, the region where multiphonon absorption plays a negligible role. The best fit curves are represented by continuous lines in Figs. 1, 2, and 4.

The value of E_g was kept fixed at 5.45 eV for all the samples and the best fit values for all the free parameters are reported in Table II together with their statistical uncertainties, which depend not only on the experimental errors but also on how strongly each parameter affects the fitting function in the investigated spectral range. The statistical uncertainties of B_2, E_m, and E_0, for the 12-μm-thick sample, are considerably larger than in the other cases probably due to the very limited available range where the second integral of the fitting function affects the results of the fit for such a sample (larger energy region). From the best fit values it can be observed that B_1 and, to a large extent also B_2, are larger for those samples with larger subgap absorption levels, consistent with an increasing population of π electronic states. The ΔE values are slightly larger than those reported in Ref. 4 (2.9–3.5 eV) and very similar to values obtained for a-C and a-C:H films (3.2–3.9 eV).[19] Moreover, the value of ΔE is found to decrease with increasing graphitic carbon content as also observed in a-C:H produced by ion irradiation.[10] For such a case in fact, the increase in the graphitic carbon component induced a shift of the shoulder feature in the spectra towards lower energies and thus produced a reduction of the pseudogap of the material. This suggests that the increase in the graphitic carbon content is also accompanied by an increase in the size of the graphitic domains.[18] The values of W, also very similar to the ones reported in Refs. 4 and 19, do not seem to be systematically affected by the amount of sp^2 carbon in the film. All these circumstances provide further evidence that the subgap absorption in CVD diamond films originates from the graphitic carbon. It is important to point out that the assumed π electronic states in the gap are adequate not only to account for the shoulder feature in the absorption spectra, typical of graphitic carbon, but also the lower-energy region (excluding the three-phonon absorption range) which has not been previously investigated and which tends to saturate into a plateau before the onset of the three-phonon absorption process.

Finally, Fig. 2 and Table II also report the results of the fitting performed on the data relative to the diamond IIa bulk sample whose values are several orders of magnitude smaller than for the CVD films. It has been suggested that the continuum subgap absorption observed in IIa diamond down to about 1 eV is similar to the one induced by neutron irradiation in diamond IIa (Ref. 20) and that in both cases it could be attributed to amorphous carbon regions.[21] We have thus attempted to fit such continuum absorption using the same hypothetical π states distribution, down to 0.6 eV, a region not previously explored in IIa diamond. The results show that the spectrum can be well reproduced with B_1 and B_2 values considerably smaller than for the CVD diamond films, a result consistent with a much smaller quantity of sp^2 carbon. Moreover, the ΔE value is larger than the one found in the case of CVD diamond. This implies graphitic carbon domains smaller than the ones found in CVD diamond, once again consistent with the substantially smaller quantity of sp^2 carbon found in single crystal IIa diamond.

CONCLUSIONS

We have carried out subgap absorption studies on very thin films of CVD diamond by means of photothermal deflection spectroscopy, a highly sensitive technique which enabled us to extend the spectral range of investigations deep into the subgap region of the material. The graphitic carbon content in the films was confirmed to be the main impurity affecting the subgap absorption and was found to increase with CH_4 concentration in the gas mixture but decreased when the substrate temperature was increased form 860 °C to 950 °C. Texturing was found to affect diamond phase purity while no systematic connection between grain size and graphitic carbon content was found. Finally the absorption spectra of the films and of IIa single crystalline diamond were found to be adequately reproduced over a very extended spectral range by a convolution integral involving only π electronic gap states associated with the sp^2 carbon.

ACKNOWLEDGMENTS

The authors are deeply indebted to the late Professor Paolo Paroli and to Dr. Marco Marinelli of the Dipartimento di Scienze e Tecnologie Fisiche ed Energetiche of the University of Rome ''Tor Vergata'' for providing the diamond films and for fruitful discussions. One of the authors (K.N.M.) acknowledges financial support from I.C.T.P., Trieste. The research was partially supported by the National Research Council.

[1] N. Amer and W. B. Jackson, in *Semiconductors and Semimetals*, edited by J. I. Pankove (Academic, New York, 1984), Vol. 21B, p. 83.

[2] U. Zammit, K. N. Madhusoodanan, M. Marinelli, F. Scudieri, R. Pizzoferrato, F. Mercuri, E. Wendler, and W. Wesch, Phys. Rev. B **49**, 14 322 (1994).

[3] M. Nesládek, M. Vanécék, and L. M. Stals, Phys. Status Solidi A **154**, 283 (1996).

[4] M. Nesládek, K. Meykens, L. M. Stals, M. Vanécék, and J. Rosa, Phys. Rev. B **54**, 5552 (1986).

[5] U. Zammit, M. Marinelli, and F. Mercuri, Rev. Sci. Instrum. **67**, 1942 (1996).

[6] D. Ritter and K. Weiser, Opt. Commun. **57**, 336 (1986).

[7] P. K. Bachmann, H. J. Hagemann, H. Lade, D. Leers, D. U. Wiechert, H. Wilson, D. Fournier, and K. Plamann, Diamond Relat. Mater. **4**, 820 (1995).

[8] S. D. Smith and W. Taylor, Proc. Phys. Soc. London **79**, 1142 (1962).

[9] J. Robertson, Philos. Mag. B **66**, 199 (1992).

[10] G. Compagnini, U. Zammit, K. N. Madhusoodanan, and G. Foti, Phys. Rev. B **51**, 11 168 (1995).

[11] P. K. Bachmann, D. Leers, and H. Lydtin, Diamond Relat. Mater. **1**, 1 (1991).

[12] M. Marinelli, A. Hatta, T. Ito, A. Hiraki, and T. Nishino, Appl. Phys. Lett. **68**, 1631 (1996).

[13] C. Wild, P. Koidl, W. Müller-Sebert, H. Walcher, R. Kohl, N. Herres, R. Locher, R. Samlensky, and R. Brenn, Diamond Relat. Mater. **2**, 158 (1993).

[14] J. F. De Natale, A. B. Harker, and J. F. Flintoff, J. Appl. Phys. **69**, 6456 (1991).

[15] G. Amato, G. Benedetto, and R. Spagnolo, Mater. Lett. **9**, 173 (1990).

[16] J. Tauc, in *Amorphous and Liquid Semiconductors*, edited by J. Tauc (Plenum, New York, 1974).

[17] G. D. Cody, in *Semiconductors and Semimetals*, edited by J. I. Pankove (Academic, New York, 1984), Vol. 21B, p. 11.

[18] J. Robertson and E. P. O'Reilly, Phys. Rev. B **35**, 2946 (1987).

[19] D. Dasgupta, F. Demichelis, C. F. Pirri, and A. Tagliaferro, Phys. Rev. B **43**, 2131 (1991).

[20] C. D. Clark, R. W. Ditchburn, and H. B. Dyer, Proc. R. Soc. London, Ser. A **237**, 75 (1956).

[21] C. D. Clark, E. W. J. Mitchell, and B. J. Parsons, in *The Properties of Diamond*, edited by E. Field (Academic, London, 1990), p. 23.